Modelling and control of a forward roll coater

Thesis for M.Sc. in Chemical and Process Engineering

by

Simon Lind

Laboratory for Process Design and Systems Engineering

Faculty of Science and Engineering

Åbo Akademi University

February 2022

Abstract

Title of the thesis:	Modelling and control of a forward roll coater
Author:	Simon Lind
Thesis supervisors:	Jari Böling *Åbo Akademi University, Turku Finland* Anders Brink *Åbo Akademi University, Turku Finland* Mika Adler *Mirka Ltd, Jeppo Finland*
Date and place:	February 08, 2022, Vasa, Finland

A roll coater applies a coating to a substrate by two or more rotating rolls. The studied case is a 3-roll forward roll coating system. The system's main objective is to apply the base coating to sandpaper. This is done by having the paper rest on a web that travels through the web and application roller. The continuous web lays on the web roller, and the coating is present on the application roller. The distance between the rollers is called the gap and will be one of the main controlling variables in managing that the correct amount of coating is applied to the paper. There are two different kinds of gaps present, one between the web and application roller and one between the metering and application roller. The one between the metering and application roller is controlling that the right amount of coating is applied to the application roller. This gap is usually run with a negative distance, meaning that the rolls are pressed together. The outer layer of the application roller is made out of deformable material to ensure that the rolls do not clash. The system is in a fully flooded regime when the gap between the web and application roller is filled with coating, and a rolling bank is present before the gap. Reducing the amount of coating in the gap will make the bank disappear, and the system will be in a starved configuration. The data for the system is collected by a sensor moving back and forth across the web's width direction.

A feedback control system is built for the coating system in Simulink. The primary control variables are the gaps between the rolls and the speed of the metering roll. A line approximation is added to represent the geometry of the rollers. An estimator is used to

ensure that data is available when the sensor is not present. The model seems to fit well when comparing simulated results to data from the plant.

Keywords: Forward roll coater, feedback control, web roll, application roll, metering roll, gap, Process modelling, simulation

Preface

This Master's thesis has been done in collaboration with Mirka. The work was carried out on distance from Vasa, Finland.

Firstly, I would like to thank Mirka for giving me this opportunity to write this thesis on this interesting topic. I would also like to thank Mika Adler from Mirka for his constant input and help during the writing process. I am also expressing my sincere gratitude to my supervisors from Åbo Akademi, Jari Böling and Anders Brink for their valuable insights and feedback throughout the thesis process.

I also would like to thank my family for their constant support and encouragement during this last year. Lastly, I would like to thank my fellow students at Åbo Akademi for making these years of my life memorable.

Simon Lind

Vasa, February 8th, 2022

Table of content

List of figures

Swedish summary – Svensk sammanfattning

I dagens läge är digitaliseringen av olika industrier ett väldigt intressant och eftertraktat ämne i och med att alla steg i en produkts livscykel kan mer eller mindre digitaliseras för att förbättra processens prestanda. Utvecklingen av modeller som ansluter den fysikaliska världen med den virtuella ökar exponentiellt i dagens värld och 2018 klassficerades dessa modeller som en av de topp tio mest eftertraktade teknologiska trenderna för kommande årtionde. Dessa modeller kallas för Digital Twins (DTs) eller digitala tvillingar på svenska. Idéen bakom digitala tvillingar är att kunna beskriva en fysikalisk process som en digital representation. Utvecklingen av digitala tvillingar går hand i hand med andra teknologier som sakernas internet (IoT, enligt engelskans ”internet of things”), molntjänster, sensorutveckling samt nya simulerings och dataanalys metoder. Det är den stora tillväxten i dessa områden som har gjort utvecklingen av digitala tvillingar möjlig. Fördelen med att ha digitala tvillingar är att kunna göra smartare beslut angående produktens livscykel, genom att analysera stora mängder digitalt framställd data istället för fysikaliska experiment. Några exempel på hur digitala tvillingar kan användas är analytiska bedömningar, predikativ diagnostik, processoptimering och för design av styrsystem. Analytiska bedömningar kan digitalt analysera processen och kan sedan implementera resultatet i den verkliga processen för att förbättra produkten. Prediktiv diagnostik kan på förhand spå när processens komponenter borde bytas ut för att optimera produktionen. Hela processen kan också optimeras genom att köra digitala simuleringar istället för att göra tester i verkligheten och detta sparar både tid och pengar.

Utvecklingen av en digital tvilling kan delas upp i fyra olika steg: (1) modellering, simulering, verifikation, validering och ackreditering; (2) datafusion; (3) interaktion och kollaboration; och (4) service. Först måste den fysikaliska modellen modelleras och simuleras för att kunna verifiera och validera om modellen stämmer med verkligheten. Steg två går ut på att hantera stora mängder verklig och virtuell data, samt sammanslagningen av dessa två. Data måste förbehandlas för att kunna filtrera och konvertera data till det önskvärda resultatet. Den processerade datan kan sedan analyseras med olika algoritmer för att undersöka systemets beteende. Det tredje steget behandlar interaktionen mellan alla olika delar av processen. En digital tvilling har interaktioner och kollaboration mellan det fysiska-fysiska, virtuella-virtuella

och virtuella-fysiska planet. Det fysiska-fysiska planet ser till att olika verkliga entiteter kan kommunicera och samarbeta för att utföra uppgifter som inte kan utföras på en maskin. Den virtuella-virtuella delen kommer att se till att olika virtuella modeller kan kopplas ihop för att dela information. Slutligen ser det virtuella-fysiska planet till att den virtuella modellen kan optimeras baserat på hur den verkliga maskinen beter sig. Dessutom kan det verkliga systemet dynamiskt uppdateras av direkta ordrar från den virtuella modellen. Det sista steget fokuserar på servicen av digitala tvillingar genom att optimera när och hur service borde utföras beroende på klientens behov. Målet med detta arbete att börja uppbyggnaden av en virtuell tvilling och kommer därmed att fokusera på steg 1. Arbetet har gjorts i samarbete med Mirka och den undersökta maskinen är ett trevalssystem som stryker ut lim för sandpapper.

Valsbestrykning är en billig och mångsidig metod att bestryka ett substrat. Huvudidén bakom bestrykning med vals är att ha två eller fler roterande valsar för att bestryka ett substrat, som ligger på en kontinuerlig webb. Uppdelningen av valsbestrykningssystem kan delas upp i två huvudkategorier beroende på om valsarna roterar åt samma eller motsatt håll. Om valsarna roterar åt samma håll kallas de för framåtkörda och om de roterar åt olika håll för bakåtkörda. I den undersökta fallet undersöks framåtkörda valsar, eftersom det är dessa som används i fabriken. Pappret eller substratet kommer att ligga på en kontinuerlig web. De tre valsarna som används kallas för tryck-, bestryknings- och doservals, beroende på vilken funktion de har i systemet. Den kontinuerliga webben ligger på tryckvalsen och denna körs oftast med samma hastighet som webben. Limmet finns på applikationsvalsen och överförs till pappret i gapet mellan tryck- och applikationsvalsen. Gapet eller nipen mellan dessa två valsar och limmängden på applikationsvalsen är de huvudsakliga styrvariabelerna som bestämmer hur mycket lim överförs till pappret. Storleken på gapet kan ställas genom att styra höjden för båda sidorna av tryckvalsen. Limmet finns i en reservoar ovanför nipen mellan bestryknings- och applikationsvalsen. Mängden lim som överförs till applikationsvalsen beror därmed på hastigheterna och nipavståndet mellan dessa två valsar. Dessa nip är väldigt små, oftast i några tiotal mikrometer och därför har applikationsvalsen ett ytterlager av gummi för att skydda valsarna från att krocka med varandra. Eftersom applikationsvalsen har ett gummilager kan nipen också köras med negativa avstånd, genom att pressa valsarna mot gummit. Detta används mellan tryck- och applikationsvalsen för att stoppa lim från att rinna igenom från

reservoaren. Flödesegenskaperna mellan applikations- och tryckvalsen kommer att variera beroende på hur mycket lim finns på applikationsvalsen. Om mängden lim är större än tryckvalsens nip kommer systemet att operera i en översvämmad regim, där ett lager av lim kommer att byggas upp framför nipen. Däremot om mängden lim är runt samma höjd eller mindre än nipen kommer systemet att köras i en svältande regim och därmed kommer limbanken framför nipen att försvinna.

Systemet kommer att behövas styras för att behålla jämn tjocklek på pappret. Limmängden ska kontrolleras både i maskin och tvärriktningen av pappret. Med maskinriktningen menas vägen som pappret går igenom valsarna, d.v.s. papprets längdriktning, och tvärriktningen innebär pappret bredd. Tvärriktningen är oftast svårare att styra i jämförelse med längdriktningen. För att kunna styra systemet måste data samlas in och detta utförs av en sensor åker fram och tillbaka i breddens riktning. Detta gör att data avläses i ett sicksack mönster, eftersom webben som pappret ligger på åker konstant framåt. Därför behövs en estimator för att beräkna vad limmängden är där sensorn inte finns.

I arbetet byggs först en simulink-modell upp för systemet för att virtuellt representera den fysikaliska verkligheten med en estimator för att beräkna vad limmängden borde vara när sensorn inte är där. Ett styrsystem konstrueras därefter för att kunna användas både för modellen och verkligheten. En linjeapproximation används för att representera valsarna och verkar bra beskriva hur systemet fungerar på grund av valsarnas geometri. Styrvariablerna som används är de båda nipen mellan valsarna, samt hastigheten för bestrykningsvalsen. Hastigheterna på de andra två valsarna inverkar också på hur mycket lim appliceras till pappret, men dessa hålls konstant med hastigheten på webben. Börvärdet på papperslimmängden styrs med nipet mellan applikations- och tryckvalsen genom att först göra en variabeltransformation till vinkeln på limmet och limmängden. Dessa två styrsignaler styrs med varsin PI-regulator och beräknas därefter tillbaka till höjden för höger och vänster sida för valsen. Höjden på valssidorna kan också kvantifieras ifall mätdata eller fysiska begränsningar finns i systemet. Med tanke på att modellen kan behövas kvantifieras har även dödzon intervall lagts till för att stoppa regleringen från att oscillera mellan två värden.

Limmängden på applikationsvalsen bestäms genom att styra det andra nipet och bestrykningsvalsens hastighet.

Modellen verifieras genom att jämföra verkliga mätningar från fabriken, genom att köra modellen med samma inställningar som fabriken hade. Verkliga värden verkar passa bra överens med vad den virtuella modellen uppvisar. Styrsystemet testas även med olika värden i tillåtna intervall, samt olika stegförändringar i den eftertraktade limmängden. Om möjligt skulle det vara fördelaktigt att göra mera tester i fabriken med förbestämda inställningar, men på grund av Covid-2019 pandemin har besök till fabriken inte varit möjliga. Nästa steg för digitala tvillingsmodellen är att börja bygga upp alla interaktioner mellan de verkliga maskinerna och den digitala modellen.

1 Introduction

The digitalization of different industries is an exciting and sought-after topic in today's world since most steps in the product's lifecycle can be improved and optimized with the help of digital means. The development of models that connect the virtual and physical spaces is increasing exponentially, and in 2018 these models were ranked in the top 10 most wanted technological trends for the coming decade. A model that connects the physical and the virtual spaces is called a digital twin (DT). The development of digital twins goes hand in hand with improvement in other technological areas, such as the internet of things (IoT), cloud-based services, sensor tech, and new and improved simulation and analysis methods. The advantage of using a virtual twin is that it can analyze and make intelligent decisions for the whole process by simulation instead of factory testing. A few areas where digital twins are used are analytical decisions, predictive diagnoses, and process optimization. By using the simulations and smart algorithms, the whole plant model can be optimized to the best settings for any wanted configuration. Predictive diagnoses will predict when a process component needs to be changed to maintain optimal performance but can also vary these decisions based on the client's needs. In general, running anything in the digital space will save both time and money compared to using factory testing. This hinges on making sure that the models used are correct and accurately represent the real world (Tao, et al., 2019).

The development of a digital twin can be split up into four steps: (1) modeling, simulation, verification, validation, and accreditation; (2) fusion of data; (3) interaction and collaboration; and (4) service. The first step will model and simulate the physical system in a virtual workspace. Furthermore, this model needs to be tested to verify and validate if it corresponds to the real-world system. The second step will involve handling all the data that will be present in different parts of the model. All the data first needs to be preprocessed by filtering and converting it into its needed form. Following this, the data can be analyzed with different algorithms to improve the system's behavior. In the third step, all different interactions between the process parts will be handled. A digital twin will involve collaboration between three different spaces, the physical-physical, virtual-virtual, and virtual-physical. The physical-physical space makes sure that different real-world entities can communicate in order to

perform more complex tasks requiring more than one machine. In the virtual-virtual space, different models can communicate and share information. Lastly, the virtual-physical space will ensure that the virtual model is correctly based on the real-world process. The actual physical system can also be dynamically updated based on information from the virtual model. The fourth service part will handle both the virtual and physical entities' maintenance by optimizing when maintenance should be performed. This thesis aims to start building a digital twin model and will, therefore, focus on step one. The work has been done in collaboration with Mirka, and the studied system is a three-roll coater, which applies adhesive coating for sandpaper (Tao, et al., 2019).

Roll coating is a cheap and versatile method of coating a substrate. The main idea behind it is to use two or more rotating rollers to apply the coating. A roll coating system can be split into two categories, depending on the roll's rotations. A forward roll coater will have the rolls rotate in the opposite direction and is the most studied configuration in literature. On the flip side, if the rolls rotate in the same direction, the roller will be in reverse mode. The studied Mirka case uses a forward roll coater, which will be the focus of this thesis. The paper rests on a continuous web, which travels through the web and application roller in order to apply the adhesive. The narrowest part of the rolls is called the gap or nip and will be the primary control variable to ensure that the specified adhesive amount is applied. The third roll is called the measuring roll and will apply the coating onto the application roller. The gap between the measuring and application rolls and their speeds will be controlled to make sure that the application roller has enough adhesive.

The system will need to be controlled to maintain an even coating on the paper. The coating thickness needs to be preserved in both the machine and cross-direction. Machine thickness is the length of the paper since this is the way the paper travels through the machine. The cross-direction is the width of the paper and is usually harder to control compared to the machine direction. In order to be able to control the system, a stream of data will constantly be fed from the sensors. The system has only one sensor that traverses the paper back and forth on a rail. This will mean that the data provided will be presented in a zigzag pattern due

to the constant movement of the web. An estimator is added to predict the data when the sensor is not present.

In this thesis, a Simulink model is built to represent the physical system virtually. A control system is then added, with the primary control variables being the two gaps between the rolls and the speed of the metering roll. The setpoint of the coating thickness is controlled by variable transforming the coating profile into the coating's angle and average thickness. A line approximation is added to represent how the rolls will behave due to their geometry. PI-regulators control the two signals before being transformed back into the rollers' left and right side signals. The amount of coating needed on the application roller is controlled by the metering roll gap and speed.

1.1 Background and control problem

The control of sheet and film processes is an exciting subject for today's industries. These processes can be sorted into metal rolling, manufacturing of paper, polymer film extrusion, and coating. For the metal industry, approximately 90% of all the produced copper, aluminum, and steel are rolled. Paper manufacturing is a sheet process and a considerable part of the paper and pulp industry. Polymer film extrusion is used in the making of different plastic products. The main goal in this thesis is to build a control system and model for a 3-roll forward roll coater that applies a base coating for sandpaper.

2 Literature review

The purpose behind coating operations is to apply an even layer to a substrate to improve the substrate's functionality, appearance, or both. Examples of common ones are hydrophobic, anti-corrosion, adhesive, and photographic coatings. Hydrophobic coatings will make a product repel water and can be used, for example, in the food industry for packaging or to make fabrics more repellant to water. Metals can be made more corrosions resistant by coating them with an anti-corrosion agent. Metal coating can be helpful if the metal is exposed to harsh climate or wet environments. Another common industry application is adhesive coatings, which are used to fasten different objects together. Paper can be coated to increase its printability or improve its visibility (Johnson, 2003).

There are many coating methods, and which one to choose depends on a variety of factors. Firstly, some coating methods will not be possible depending on the coated part's shape, size, and accessibility. For example, a more advanced three-dimensional product will not be able to be roll coated. More factors such as the production speed requirement, labor and equipment cost will need to be investigated when choosing the most suitable method. Fast automated methods, like roll coating, will be superior to hand application if many products are being manufactured. However, if the production volume is low and spread out, hand applying might be cheaper than investing in a roll coating machine. Coatings will have different open and curing times. Open time means how long the coat is still workable after it has been applied. Flammability, noxiousness, and viscosity of the coating will also affect the choice of coating method. Lastly, depending on the rheology and characteristics of the coating used, some methods will be more suitable. Rheology is the study of the deformation and flow of both solid and liquid materials (Cognard, 2006).

2.1 Roll coating

Roll coating is an inexpensive and versatile method of coating a specific substate. The main idea behind roll coating is to use two or more rotating rolls to apply a thin coating film onto a continuous web. Roll coating setups can be classified into two main categories, depending on the rolls' rotation. In forward roll coating, the rolls will rotate in the opposite direction, and

the fluid motion through the nip is going in the same direction, illustrated on the left in Figure 1. The place coating rolls are closest together is called the nip, but gap is also used in literature. Reverse roll coating occurs when the rolls rotate in the same direction and cause the two roll surfaces to move in opposite directions, as seen on the right in Figure 1. Usually, reverse roll coaters are more versatile than forward roll coaters due to handling more viscous coats at higher speeds, but they are also more expensive and complex. In this thesis the object of study is a forward roll coater (Kapur, 1999).

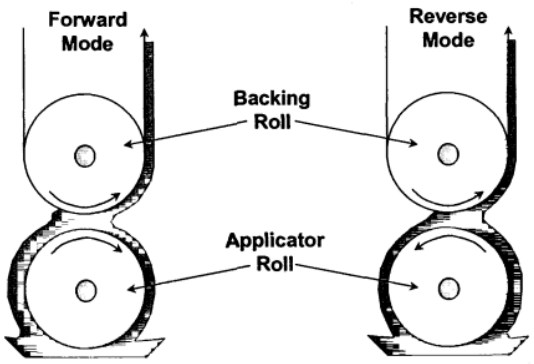

Figure 1: Forward and reverse roll coating (Johnson, 2003).

2.2 Forward Roll Coating

Forward roll coating is used for web speeds between 3 and 60 m/min with a usual coating viscosity ranging between 1-50 mPas (Kapur, 1999). The forward roll setups are illustrated in Figure 2, on the top as a pan-fed three-roller system (a) and on the bottom as a reservoir fed four-roller system (b). The roll called the back-up or web roll is driving the substrate web and is usually made from solid steel. The application roll's role is to pick up the coating from a reservoir and move it to the nip region between the web and application roll. This roll can be covered in an elastically deformable roll cover to avoid steel rolls from clashing. The advantage will then be that the coating can be made much thinner without worrying about roll clashing. In the upper figure (a), the pick-up or metering roll is partly submerged in the feed pan to pick up the coating and apply it to the application roll. Comparatively, in the lower figure (b), the coating is contained in a reservoir above the two outer rolls' nips (Carvalho & Scriven, 1997).

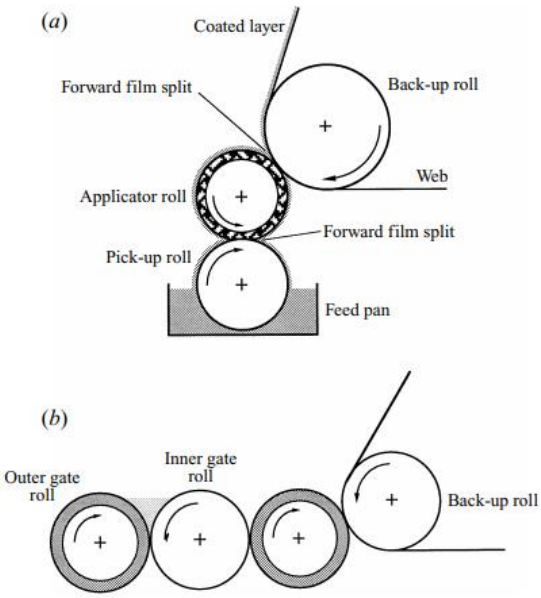

Figure 2: Forward roll coating examples (Carvalho & Scriven, 1997).

2.2.1 Positive gap and negative gaps

A roller system can run with a positive or negative gap. Positive gaps imply that both rolls' center distance is larger than their combined radii. This gap is the most studied setting in literature and is used in many industries. The gaps are usually larger than 25 micrometers for rigid steel rolls to avoid clashing between the rolls, but this is not a problem for deformable rolls because of the elasticity. For a deformable roll system, the larger the gap becomes, the more like two rigid rolls, the system will behave since less force will be applied to the deformable roll and the roll will therefore not compress as much. Reversely, the distance from the center of the rolls is smaller than the combined radii for a negative gap. Negative gaps are only possible with deformable rolls since otherwise, the rolls would clash together. The gap between the rolls can either be a fixed gap or a load-controlled gap. A fixed gap means that the gap is set to a specific height, while a load-controlled gap means that a specific load is applied to one of the rolls and will then settle into a particular gap height depending on the elastic properties of the rolls (Kapur, 1999).

2.2.2 Roll flow regimes

Furthermore, roll coaters can be classified depending on the rolls' flow regime. A roller operating with a thicker inlet film than the gap ($H_{in} > H_{Gap}$) is called a flooded regime or classical roll coating and will cause a rolling bank of coating fluid upstream from the gap. This operating mode is the most studied and well understood. On the flip side, the rolling bank will disappear when the coating input is lowered, which will cause the roller to operate in a starved configuration ($H_{in} < H_{gap}$) (Abbott, et al., 2011).

2.2.3 Fully flooded regime

The pressure distribution for a fully flooded regime will be calculated using the lubrication approximation. This is due to the fluid in the nip can be seen as one-dimensional because of the converging and diverging nature of the flow. The inlet side will generate high pressure from the squeezing motion of the fluid and the outlet side will cause sub-atmospheric pressure due to the diverging flows. However, the flow fields are not one-dimensional and needs to be determined with computational methods.

The flow in the gap for a fully flooded regime can be split into two parts, a rectilinear flow through the gap and a two-dimensional flow further down where the film splits. In the gap region, the pressure distribution is given by the lubrication approximation from (Carvalho & Scriven, 1997)

$$\frac{dP}{dX} = \frac{12\mu}{H(X)^3}[\overline{U}H(X) - Q]$$

where P is the pressure distribution, μ is the liquid viscosity, X is the horizontal distance along the gap, U is the average surface velocity of the rolls, H(X) is the clearance between the rolls and Q is the flow rate through the gap. The average surface velocity can be calculated as

$$\overline{U} = (U_A + U_B)/2$$

with U_A and U_B being the edge velocity of the web and application roll. The edge speed ratio S depends on the edge velocities by S = U_A / U_B with S > 0 for forward roll coating and S < 0 for reverse rolling. The local clearance can be seen below

$$H(X) = H_A(X) - H_B(X) = 2H_0 + \frac{X^2}{R} + D(X)$$

where H_A and H_B are the gap distances to a reference plane tangent to the rigid roll, as seen in Figure 3. The clearance or gap between the two undeformed rolls is H_0. The deformable rolls local displacement is

$$D(X) = \frac{1}{K}P(X)$$

where K is the spring constant and depends on the rolls deformable cover properties: layer thickness L, elastic modulus E, and Poisson's ratio v. The model does not work on incompressible materials with Poisson's ratios of v = 0.5. The roll's effective radius R is given by

$$\frac{1}{R} = \frac{1}{2}\left(\frac{1}{R_A} + \frac{1}{R_B}\right)$$

where R_A and R_B are the individual rolls radii (Carvalho & Scriven, 1997).

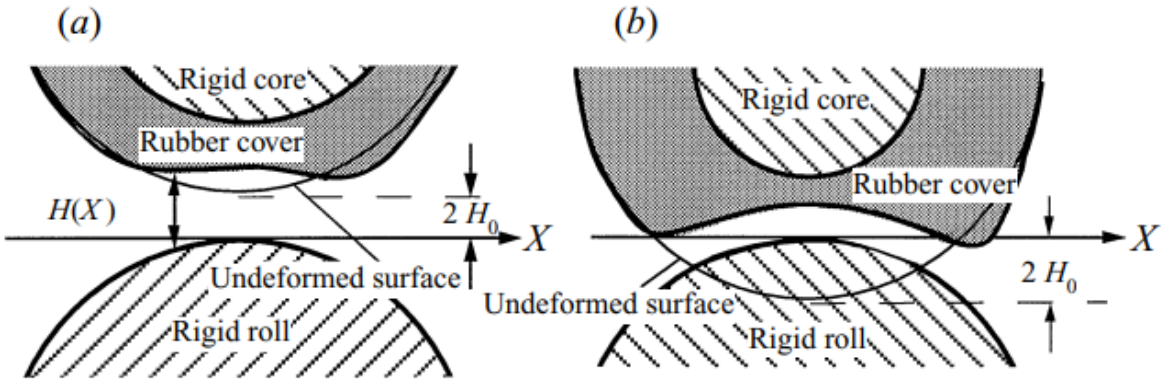

Figure 3: Deformable roll gaps. (a) Positive gap. (b) Negative gap (Carvalho & Scriven, 1997).

The flow field for a typical forward roll coater with a flooded regime can be seen in Figure 4. The lines in the figure can be seen as "streamlines" meaning the path a particle travels along with the flow. As seen below the flow close to the nip is very linear, while the flow before and after the nip will recirculate.

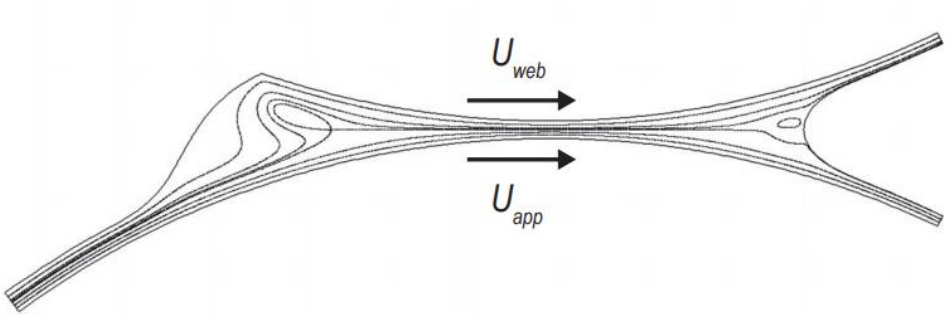

Figure 4: Typical flow field for a fully flooded forward roll coater (Abbott, et al., 2011).

The flow rate for a fully flooded forward roll coater have been calculated to

$$Q_{fully\_flooded} = \frac{(U_A + U_B)}{2} \cdot H_{gap} \cdot \lambda_{flooded}$$

Where the $\lambda_{flooded} \approx 1.34$ and $Q_{fully\_flooded}$ is the flow rate between the rolls per unit length (calculated in m^2/s). H_{gap} is the nip distance and U_A and U_B is the speed of the rolls. To preserve the mass balance, this means that $H_{in} > 1.34 \cdot H_{gap}$. To preserve a continuous flow balance the following flow equation per unit length is proposed for a flooded regime when the incoming coating thickness H_{in} is between $1.34 \cdot H_{gap}$ and H_{gap}

$$Q_{flooded} = \frac{(U_A + U_B)}{2} \cdot H_{in}$$

Here the λ term would then be 1. The film split ratio H_{ratio} is the ratio between how much coating is transferred to the web H_{web} with regards to being left on the application roller H_{app}. The following equation is used for film split ratio H_{ratio}

$$H_{ratio} = \frac{H_{web}}{H_{app}} = \frac{S(S+3)}{(1+3S)}$$

Where S is the speed ratio between the rolls, as mentioned earlier. If the speed of the rolls is the same (S = 1), the film split ratio will be 1, i.e., an even split of the film (Abbott, et al., 2011) (Thompson, 1992) (Gaskell, et al., 1998).

2.2.4 Fully flooded forward roll coater operating window

The optimal operating window for a fully flooded forward roll coater with quite high viscosity fluids was determined by (Coyle, 1997) and presented in Figure 5. The coating will have air entrainment in the reservoir when the application roll speed is much faster than the web speed due to the run-back. This is due to the excessive amount of coating that the application roller will pick up. Ribbing will affect the process at high web speeds, which means that the coat will not be even but have a sinusoidal wavy pattern instead. This is discussed more in detail later in the thesis. Starvation will occur when the application speed is low in comparison to the web speed (Abbott, et al., 2011).

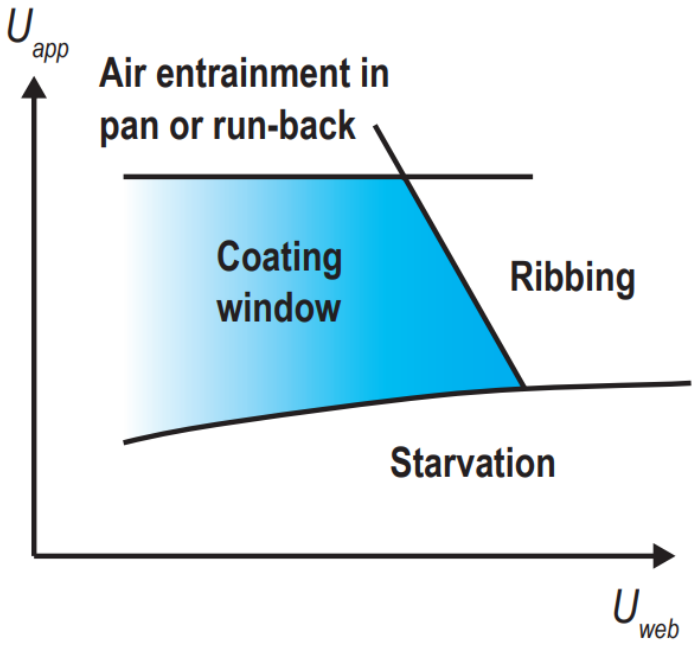

Figure 5: Operating window for a fully flooded regime (Abbott, et al., 2011).

2.2.5 Starved regime

For a starved regime, the incoming coating thickness will be less than the gap between the rolls. This will cause the rolling bank present in the fully flooded scenario to disappear. The following flow rate equation is proposed for a starved regime, when H_{in} is between H_{gap} and $H_{gap} \cdot \frac{k-1}{k-0.3}$

$$Q_{starved} = \frac{(U_A + U_B)}{2}(H_{gap} - (H_{gap} - H_{in})k)$$

where the constant $k > 1$ and will determine when the regime will change to an ultra-starved configuration, meaning that H_{in} is smaller than $H_{gap} \cdot \frac{k-1}{k-0.3}$. For example, when k = 1.3, the regime change between a starved and an ultra-starved regime occurs at $H_{in} = 0.3 \cdot H_{gap}$. The flow rate for the ultra-starved regime is based on (Gaskell, et al., 1998)

$$Q_{ultra\_starved} = 0.3 H_{in} \frac{(U_A + U_B)}{2}$$

The minimum $\lambda = 0.3$ is established by (Gaskell, et al., 1998) and it is the same term used in the denominator for the $\frac{k-1}{k-0.3}$ term to ensure that the flow changes linearly, when λ goes from 1 to 0.3.

The film split ratio is based on (Landau & Levich, 1942)

$$H_{ratio} = \frac{H_{web}}{H_{app}} = S^{2/3}$$

The typical flow field for a starved forward roll coater is shown in Figure 6 and is mainly two-dimensional with recirculating flows. The streamlines are now recirculating more than the fully flooded scenario and are also occurring in most of the flow area. The liquid is transported to the web by transfer jets that whirl around (Abbott, et al., 2011) (Thompson, 1992) (Gaskell, et al., 1998).

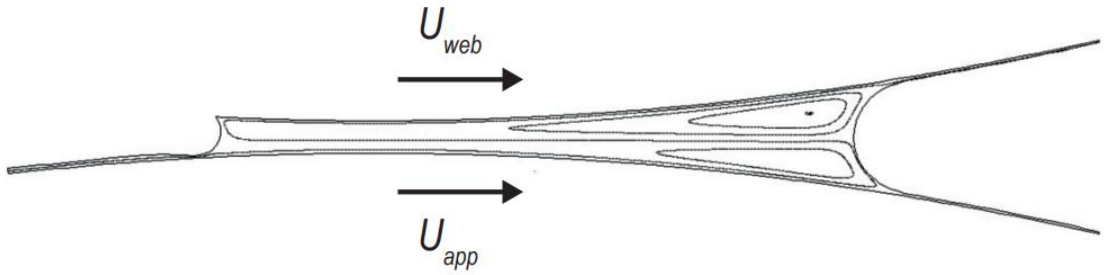

Figure 6: Flow field for a starved forward roll coater (Abbott, et al., 2011).

2.2.6 Starved roll coater operating window

The operating window for a starved forward roll coater was also determined by (Coyle, 1997) and is shown in Figure 7. As seen in the figure if the application speed is too low the bead will break and cause starvation. On the other hand, if the application speed is too fast the input bank might become unstable. Lastly, if S is too large, i.e., the web speed is much higher than the application roll speed, air entrapment could cause problems.

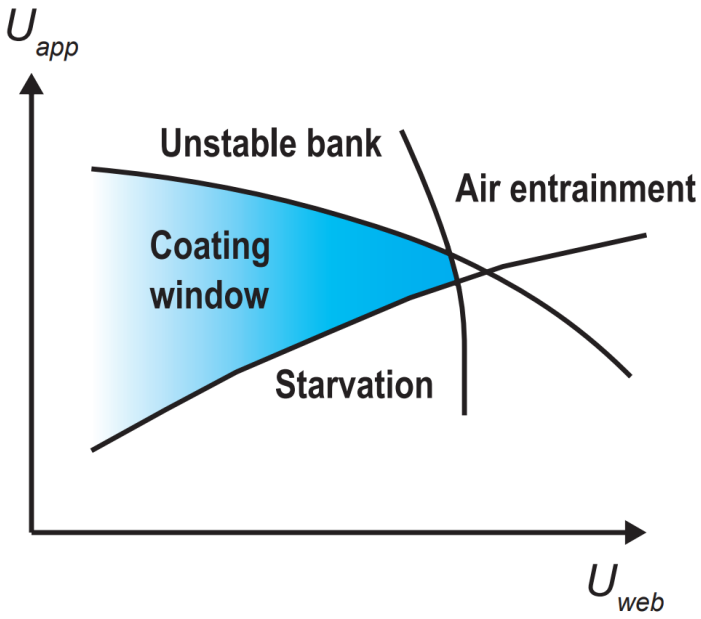

Figure 7: Operating window for starved forward roll coating (Abbott, et al., 2011).

2.2.7 Transition between starved and flooded regimes

A summary of the regimes based on the value of H_{in} with k chosen at 1.3 can be seen below

Ultra-starved regime: $0.3 \cdot \mathrm{H}_{gap} > H_{in} \geq 0$

Starved regime: $H_{gap} > H_{in} \geq 0.3 \cdot \mathrm{H}_{gap}$

Flooded regime: $1.34 \cdot H_{gap} > H_{in} \geq \mathrm{H}_{gap}$

Fully flooded regime: $H_{in} \geq 1.34 \cdot H_{gap}$

Figure 8 illustrates the changes in the flow rate according to the flow equations mentioned above. The units used are not of importance since the point is to show the general flow rate changes when H_{in} is increasing. The speed of the rolls and the H_{gap} are all set to 10, with the H_{in} starting at 0 and increasing up to 20. The regimes in the figure are as follows

Ultra-starved regime: $3 > H_{in} \geq 0$

Starved regime: $10 > H_{in} \geq 3$

Flooded regime: $13.4 > H_{in} > 10$

Fully flooded regime: $H_{in} \geq 13.4$

This example assumes that the web is always in contact with the application roller, which might not be the case when the difference between H_{in} is small compared to H_{gap}. The flow rate increases more or less linearly in the starved and flooded regimes. In the fully flooded regime, increases in H_{in} no longer increase the flow since it is limited by the size of the gap. If the amount of coating on the application roller is not measured by any sensor, it can be hard to determine what regime the coater is running in. An estimate of the application roller coating thickness is presented in the following chapter (Abbott, et al., 2011) (Gaskell, et al., 1998) (Thompson, 1992).

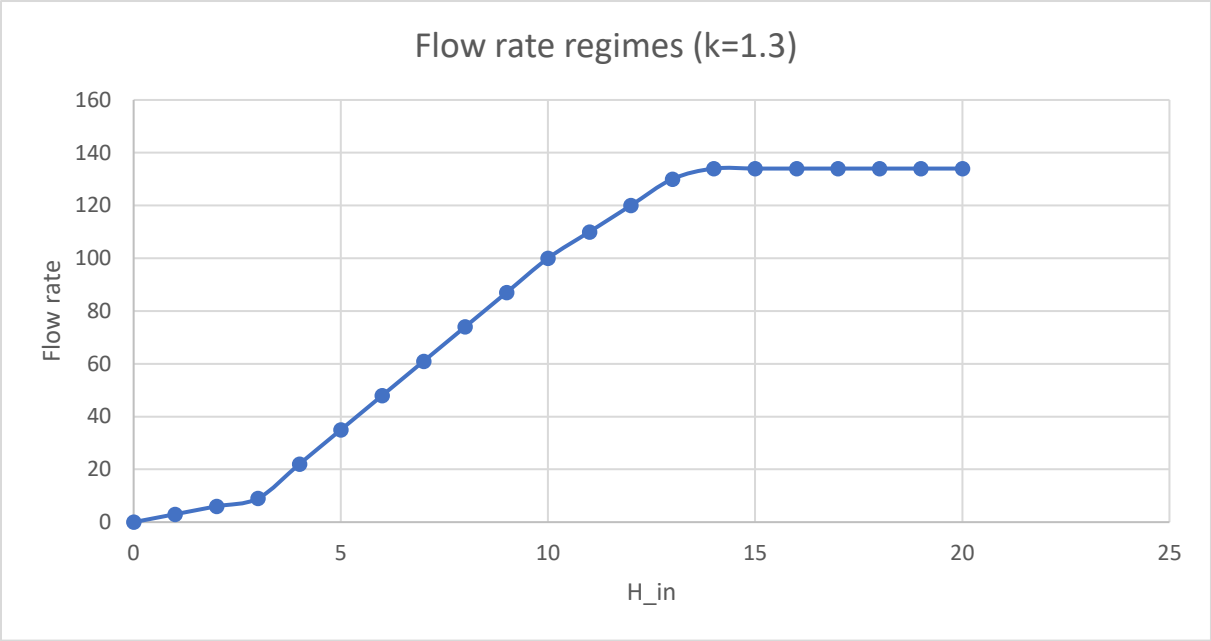

Figure 8: Flow rate depending on H_{in} for general forward roll coater. The gap and roll speeds are set to 10.

2.3 Negative gap model

As mentioned earlier, negative gaps are present when the distance from the center of the rolls is smaller than the combined radii of the rolls. One of the rolls will have to have a deformable layer *b* to prevent the rolls' clashing. The distance of the negative gap, i.e., how much one roll is pressing into the other, will vary depending on the thickness of the deformable layer. The following empirical model has been found for a forward roll coater using a negative gap

$$H \approx 0.4(\mu\bar{V})^{0.6}W^{-0.3}E^{-0.3}R^{0.7}$$

Where H is the coating thickness, μ is the fluid viscosity, $\bar{V}$ is the speed of the roll, W is the load on the rolls, E is the effective elastic modulus, and R is the radius of the rolls. The applied load W is calculated from Hooke's law according to

$$W = -kx$$

$$k = \frac{EA}{L}$$

Where k is the spring constant, x is the negative gap between the rolls, A is the affected area and L is the length of the roll. From studies, it has been shown that the deformable cover thickness b has a negligible influence as long as $b > \frac{\delta}{2}$ where δ is the contact width. The contact width is the height of the area pressing into each other and is presented in Figure 9 below (Cohu & Magnin, 1997) (Johnson, 2003) (Abbott, et al., 2011).

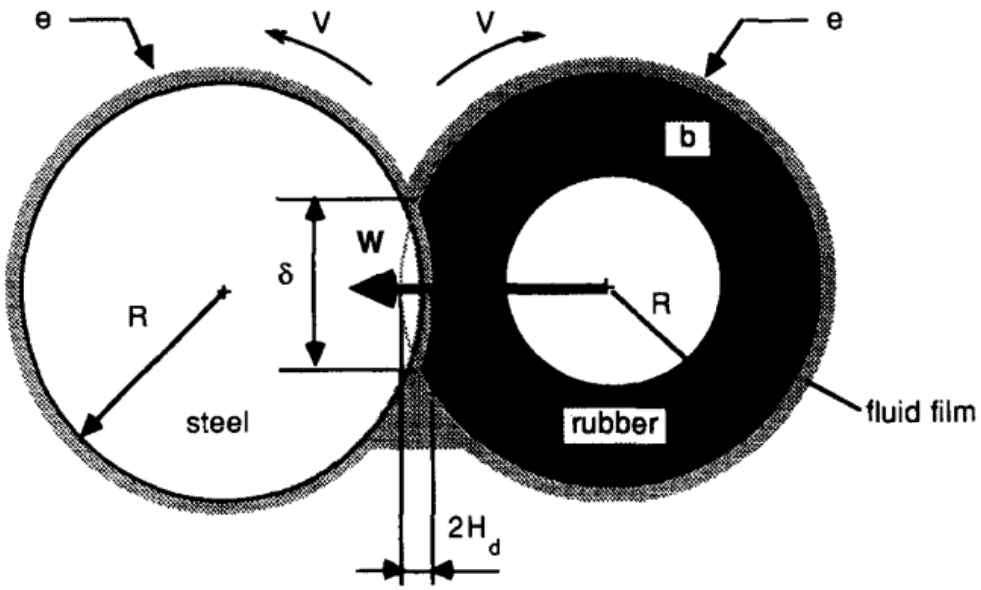

Figure 9: Forward roll coater with negative gap (Cohu & Magnin, 1997).

2.4 Cross-directional Control

The main control objective for the above-mentioned processes is to maintain the uniform thickness and properties of the sheet or film. This can further be split into control in the machine direction (MD) and cross direction (CD) of the product. The machine direction is the way the film or sheet is traveling through the machine or the length dimension and is illustrated in Figure 10. The product's width is called the cross direction and is usually more difficult to control than the MD.

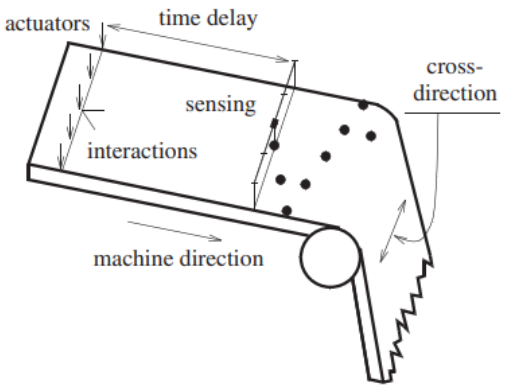

Figure 10: Typical description of film or sheet process (VanAntwerp, et al., 2007).

The most common processes using cross-directional control are papermaking, metal rolling, coating, and polymer extrusion. These processes' control is handled in the distribution device, called die in coating and polymer extrusion, work roll in metal rolling, and headbox in paper machines. The actuators in the distribution device are usually evenly spaced along the CD. The headbox will have multiple slice lip actuators evenly spread along the width for paper machines to control the surface weight. Coating and polymer film applications use screws or bolts as actuators to control the flow through the die. Metal rollers have varying pressure across the width of the work roll to control the thickness of the metal sheet. In some processes the coat thickness is set by lowering and increasing the height of the left and right side of the roll. This will mean that the degree of freedom is lower than having actuators across the whole width. For example, if the roll is not a perfect cylinder but more like a cone, this can be controlled by setting the sides. However, if there is a local disturbance, for example, a dent or manufacturing error in the roll, this will continue to cause an uneven coat. Comparatively, local errors are more easily handled in a process with more actuators. On the flipside having more actuators, in some cases, several hundred will cause the control problem to become a lot more complex in comparison to just having a few actuators (VanAntwerp, et al., 2007).

2.5 Sensors

To control the specified characteristics of a wanted product, sensors are needed to gather the necessary data. The sensors are high-cost items and often, only a few sensors are used. A good

result with only one sensor can be achieved by having the sensor move back and forth on a rail orthogonal in relation to the direction of the sheet's MD. The resulting sensor data will be presented in a zigzag pattern due to the movement of the sensor combined with the sheet moving. An estimator can now be used on the collected data to get an estimate across the whole sheet. The estimator used in this thesis is presented in Chapter 3.7. Another approach is using multiple static sensors to gather the full profile instantly. This will be more expensive but will yield a much more considerable amount of data. While a bigger pool of measurement will give a more accurate profile, it will also require more computing power to be able to do all the needed calculations to control the system between each sampling instance (VanAntwerp, et al., 2007).

2.6 Instabilities

During the operation of any coating process, various instabilities or defects can occur. Instabilities are usually classified as constantly reoccurring variations in the film thickness properties instead of a more randomly spaced defect that might only appear on a specific part of the film. One of the most common instabilities is ribbing, which will be discussed below (Chong, et al., 2007).

2.6.1 Ribbing

As stated earlier, any coating process's goal is to produce a uniform flat film across the substrate. However, it has been observed that the film is often applied in a wavy sinusoidal pattern across the whole web width. This is called ribbing, but the literature also uses corduroy or rake-line. The effect is present in both forward and reverse roll coaters, negative and positive gaps, and is a challenge for the whole industry. Ribbing occurs because of differences in the stabilizing surface tension and the destabilizing pressure gradient present on the nip's downstream region. Most research regarding ribbing phenomena has been focused on finding the critical capillary number Ca*, for which ribbing will occur. In other words, as long as the capillary number (Ca) is lower than the critical capillary number Ca*, no ribbing should appear.

For positive gaps, faster roll speeds will increase the capillary number (Ca) and lead to more ribbing. However, increasing the gap between the rolls will increase the value of Ca* and give a bigger buffer before ribbing occurs. It has also been shown that using a rigid-deformable roll pair will lead to higher Ca* values compared to using rigid steel rolls. This is mainly observed at lower gap heights compared to more significant gaps. The reason is that the pressure on the deformable roll layer will be lower at large gaps, and the roll will behave more like a rigid roll. The pressure between the rolls will be higher at smaller gaps and change the coating's fluid profile. The downstream film split meniscus will move further away from the nip, giving a stabilizing effect. Thicker elastic coverings can also handle larger deformations and will give a higher Ca* value.

When roll pairs are operated with negative gaps, ribbing has been shown to always be occurring and it is then a matter of controlling the wavelengths of the ribs. The more negative the gap becomes, the higher the loading pressure will be between the rolls and this decreases the ribbing wavelength and lead to narrower ribs. Regardless of what gap setting is used, increasing the roll speed will lead to a larger rib wavelength and will take longer to level out. Therefore, it is a decision between having a higher production rate with ribbing occurring versus higher quality but a slower process (Chong, et al., 2007).

3 Method

3.1 Research objective

This thesis aims to represent and control the forward roller system in a virtual model to be used as a digital twin. The model of the roller system is built on published literature, which is presented in Chapter 2 of this thesis. Various control methods are applied to control the system and are shown below. The model and control system is created in the simulation software Simulink.

3.2 Mirka physical system

A three-roll setup is used with a reservoir fed system in the studied Mirka case. The application roll is covered with a deformable layer with the neighboring metering and web rolls being made from steel. To control the nips between the rolls, the application roll is locked into place with the web and metering roll moving to set the correct gaps.

The gaps are fixed gaps, so a specific gap is set by controlling both sides of the web and metering rollers. Both sides' height settings will usually be set to the same height to assure an even coating, assuming that the rolls are flat and without defects. If the roll got manufacturing defects, for example, if the roll is more like a cone than a perfect cylinder, the height can differ between the sides to make the coating even. The gap between the application and web roll operates with a positive gap, usually with a gap greater than 100 micrometers because of the paper's thickness. The gap between the application and the metering roller is negative. Utilizing a negative gap will prevent the liquid coating resting in the reservoir between both rolls from flowing through the gap due to gravity. The specific gap will depend on the elastic properties of the deformable application roll.

Only one sensor is used to measure the coating profile. The sensor moves back and forth on a rail and will record the data in a zigzag pattern.

From a controlling point of view, the main objective is using different control strategies to control the amount of base coat applied. In the studied case, the degrees of freedom are lower than other cross-directional processes due to only controlling the right and left side heights and the speed of the metering roll.

3.3 Model

The model for the above-mentioned system is built in Simulink to be able to control it. Different control ideas are implemented based on whether the system is fully-flooded or starved. Mika Adler from Mirka initially modeled the physical model. This thesis work is based on his model, focusing on the control strategies. The model is based on the theory presented earlier in the thesis. The control strategies will be presented below.

3.4 Control variables

For the control of the above-mentioned system, the main control variables will be the web roller gap and will be set by two different actuators for the right and left sides. This will be the main determining factor in achieving the correct coating thickness. The other essential variables will be the speed of the metering roll and the gap between the application roller and the metering roll to ensure that enough coating is on the application roller. The regime will depend on how much coating is on the application roller compared to the web and application gap.

Other variables that will affect the process are the speed of the web and the application roller. These will often have the same speed to ensure that no shear forces are present. The web speed will be controlled by a separate actuator and will also be set to match the speed of the web and the application rollers. Lastly, the fluid properties will affect how the coat will behave. The fluid viscosity will be the main one and will depend on what kind of coat is used and its temperature. The fluid viscosity will be set as a constant for this model because a separate system in the plant automatically controls it.

3.5 Line approximation

The first control strategy implemented is a line approximation of the base coat applied to the web. Sensors will gather the coating profile and assuming that the rolls are flat, the coat can be seen as a line. Instead of using the whole profile, a linear approximation will be implemented. An offset of the starting and ending point will be used to stop side overflow from affecting the result. The specific method used in this thesis is the least-squares and is being solved in Matlab. A linear system can be seen as the following

$$y = \beta_0 + \beta_1 x$$

where β_0 is the y-intercept and β_1 is the slope of the line. With n observed values the system can be presented in matrix form Y, X and β as below

$$\begin{bmatrix} y_1 \\ y_2 \\ \vdots \\ y_n \end{bmatrix} = \begin{bmatrix} 1 & x_1 \\ 1 & x_2 \\ 1 & \vdots \\ 1 & x_n \end{bmatrix} \begin{bmatrix} \beta_0 \\ \beta_1 \end{bmatrix}$$

The least-squares method aims to minimize the sum of the squared residuals S. Residual r is the difference between the data and the model.

$$S = \sum_{i=1}^{n} r_i^2 = \sum_{i=1}^{n} (y_i - \hat{y}_i)^2$$

Where y_i is the observed data and $\hat{y}_i$ is the fitted response for the model. The β vector can be solved by

$$\beta = (\mathrm{X}^{\mathrm{T}} X)^{-1} X^T Y$$

or in Matlab by the backslash operator $\beta =$ X\Y (Wells & Krakiwsky, 1971) (MathWorks, 2022).

3.6 Variable transform

After implementing the line approximation, the profile will be variable transformed. The start and ending points of the line are variable transformed into average coating thickness and height difference. An even coat can be achieved by setting the set point of the height

difference to 0. This will mean that one PI regulator will try to even the coat and the other will control the desired coating thickness. For this to work, the assumption is that the rolls are flat. Another thing to note is that even if surface defects affect the profile, not much can be done if they are in the middle of the rolls. The average coating thickness is calculated as below:

$$U_{Coat\_average} = \frac{h_{Coat\_left} + h_{Coat\_right}}{2}$$

Where h_{Coat_left} and h_{Coat_right} is the left and right side starting points taken from the line approximation (Häggblom & Böling, 2013).

3.7 Estimator

As mentioned earlier, the measured coating profile will be presented in a zigzag pattern due to the movement of the web and the sensor. This means that in order to get a complete coating profile, an estimator is implemented. The idea is that the estimator will assume how the coating profile will look when the sensor is not there, based on previous data. Assuming the system is a first-order system with the following dynamics:

$$\hat{y}(k+1) = a\hat{x}(k) + bu(k)$$

$$a = e^{-h/T}$$

$$b = K(1-a)$$

Where h is the sampling time, T is the time constant, and K is the gain. Then the following estimator can be used.

$$\hat{x}(k+1) = a\hat{x}(k) + bu(k) + k(y_m(k+1) - \hat{y}(k+1))$$

Where y_m is the measured value, $\hat{y}$ is the difference between the measured and estimated value, and k is a constant between $0 \leq k \leq 1$ (Häggblom & Böling, 2013).

3.8 Split Range

Split range control is implemented when the roller is operating in a fully flooded setup to control the amount of coating transferred between the metering and application roll. This means that one controller will control both the speed of the metering roll and the gap between the metering and application roller. If the controller output is between 0 – 30 % the gap will be controlled and the remaining 70% will operate the speed of the roll. This split is designed to give a linear response to ensure good control properties.

3.9 Quantified data

In scenarios where the data or the physical system is quantified, i.e., when the physical limitations of the system makes it only take specific values, dead zones can be implemented. At the beginning of this work, it wasn't confirmed if the actuators setting the height of the rolls was quantified or not. The solution was to add a dead zone to the controller. This means that when operating in ranges between two quantified values, the difference between the actual value and desired value, i.e., the error signal will be set to 0. The main advantage of this approach is to stop the system from oscillating between values when the setpoint is between two of the quantified values.

4 Results

4.1 Simulation results

The data results have been represented by running different simulations with different parameters to ensure that the system is stable and behaving as envisioned. The parameters used are mainly the same and will be disclosed to clarify the specific result. Simulations have been the main focal point to test the viability of the model and controller. A bit of data has been taken from the actual plant to compare it with the simulation result, but more data is needed to reach more thorough conclusions.

4.2 Simulation assumptions

The results of these simulations are based on a few assumptions. Firstly, constant fluid viscosity is assumed but may vary depending on the temperature and properties of the fluid. This is mainly because a separate system regulates the temperature to keep the temperature of the coat at a constant level. Therefore, assuming constant fluid viscosity should not significantly impact the result.

Secondly, the rolls are assumed to be even and cylindrical. Minor defects may be present on the rolls, but these are negligible in the grand scheme of things. The effective elastic modulus and the thickness of the deformable application roller are also assumptions. Assuming the layer thickness should be fine since the impact of the thickness is negligible, as explained in Chapter 2.3. The effective elastic modulus assumption is based on the properties of the layer material and should be close enough to ensure good results.

Another thing to note is that it is hard to say what regime the actual roller is being run in because the coating thickness on the application roller is not measured but estimated from the speed of the metering roll and the negative gap estimation presented in Chapter 2.3.

4.3 Simulation parameters

As mentioned earlier, the parameters are mainly the same throughout the simulation runs and will be mentioned separately if changed. The speed of the web, application roller and moving web is chosen to be 1:1 at a speed of 55 m/min. The metering roll speed is set to half of the application roll speed for the starved configuration but varies in the fully flooded one. The viscosity in the simulations is set to $0.097\ Pa \cdot s$, unless otherwise stated.

4.4.1 Startup simulation

The result of the first simulation is presented in Figure 11 and is based on the fully flooded scenario with a coating thickness setpoint of 8 g/m^2. The top left figure shows one width profile taken by the sensor from one vertical sweep. The data point got Gaussian noise added to each measurement to simulate general plant noise. The blue line is the line approximation done by the least square method, as presented in Chapter 3.5. A three-dimensional plot of the coating thickness on the paper is shown in the top right corner. The x-axis represents the width of the track in centimeters, with the y-axis showing the time and the z-axis the surface weight measured in g/m^2. The middle figure shows the coating thickness on the application roller and the web roller's left and right side height, as one line due to them being the same height. The application roller's coating thickness is set to be 1.7 times the height of the web gap to ensure that the roller is running in a fully flooded configuration. The bottom figure shows the mean coating thickness across the full-width profile.

A starved simulation is run in Figure 12 with the coating thickness setpoint of 6 g/m^2. The top left figure shows the negative gap between the metering roll and application roller. The top right figure shows the coating thickness in a three-dimensional figure, just like in the fully flooded simulation above. The middle plot represents the coating thickness on the application roller and the web gap. Compared to the simulation above, the web gap is larger than the application roller coating thickness since it is running in a starved configuration.

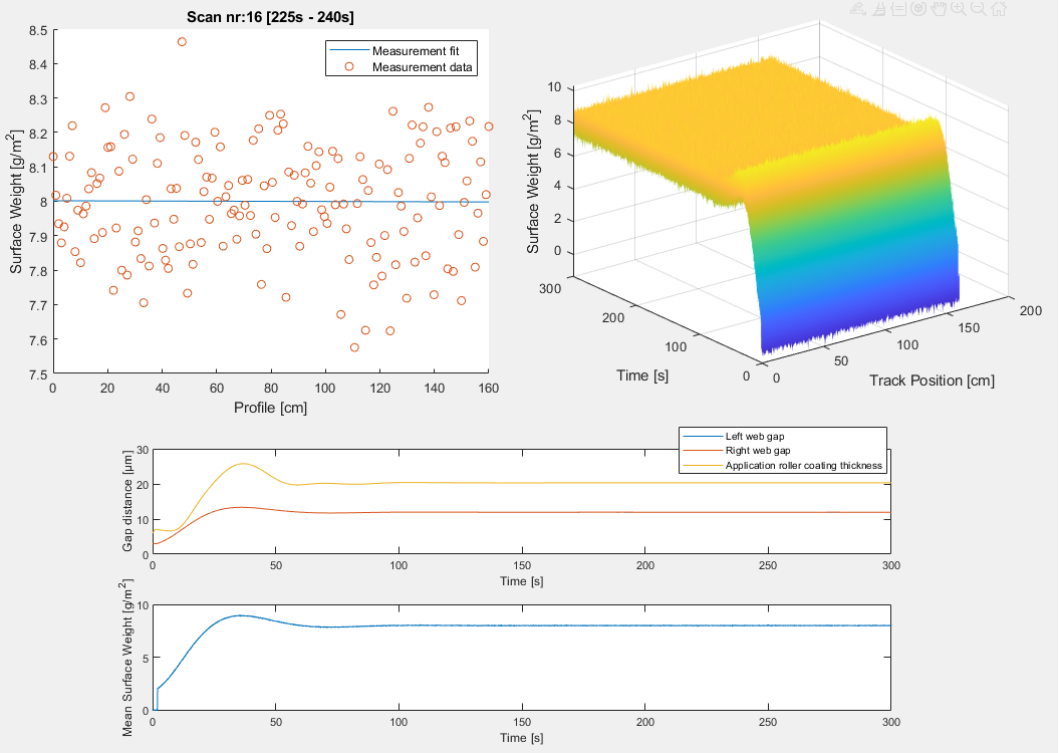

Figure 11: Simulation for a fully flooded roll coater with the coating thickness setpoint of 8 g/m².

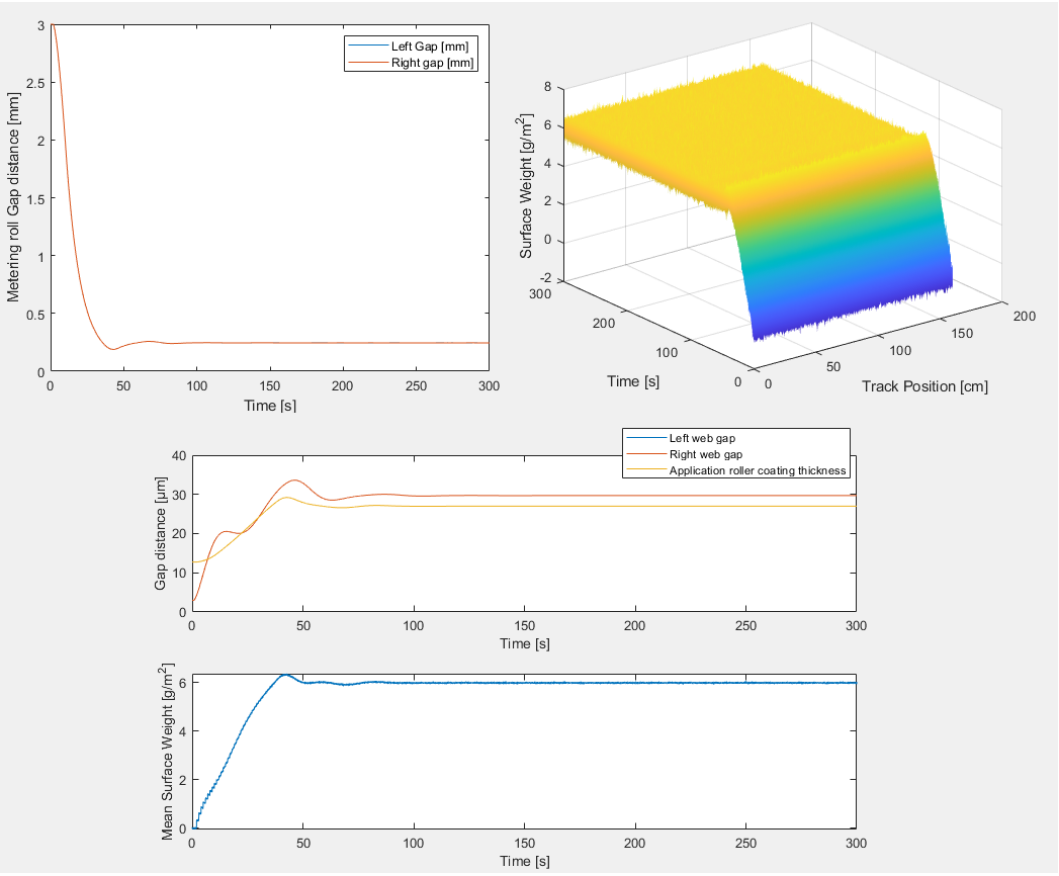

Figure 12: Simulation for starved roll coater with the coating thickness setpoint at 6 g/m².

4.4.2 Uneven rolls

The data presented in Figure 13 is based on the fully flooded roll coater simulation. The speed is the same as earlier, but the right side of the web roll got a height offset of $5\ \mu m$ to represent the roller not being a perfect cylinder. Therefore, the roller can be seen as more cone-like than cylindrical. This offset is most likely too big of a discrepancy to appear in plant scenarios but is used to illustrate the ability of the controller to handle uneven rolls. The top figure shows the web roller's side heights and the application roller coating thickness, with the bottom figure showing the coating thickness profile. The figures show that the coating will be uniform, even though the height varies on the left and right sides.

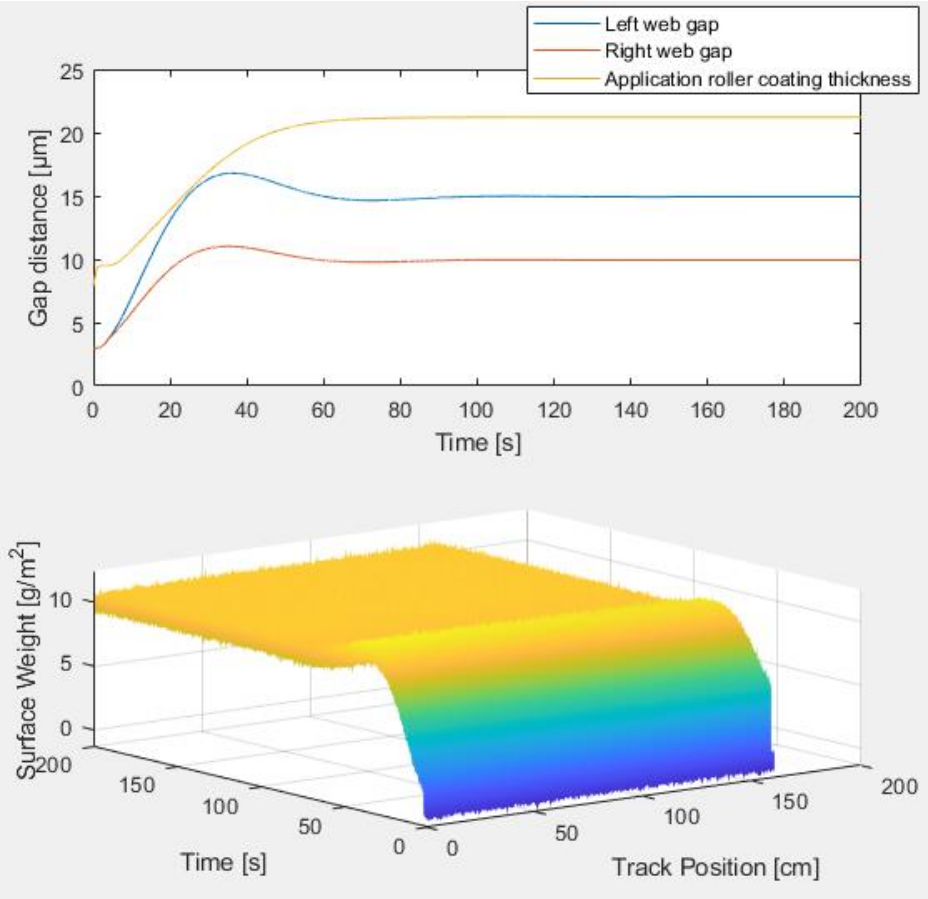

Figure 13: Fully flooded Simulink simulation with uneven rolls; right roll got a 5 µm offset.

4.4.3 Coating Thickness limits

The next simulation shown in Figure 14 is also based on the fully flooded configuration. The top figure shows the gap and application roller coating thickness with the bottom showing the mean coating thickness on the paper. This figure shows the minimum and maximum coating thickness achievable with the max roller speed. The max coating thickness achieved here is 17 g/m^2 and the minimum as 2.4 g/m^2. For this scenario the most interesting result is the max one since the minimum can be lowered by reducing the speed of the rollers. The metering roll gap is operating between -3 mm and -0.2 mm, and these are the limiting factors on the coating thickness. The web gap can always be made bigger or smaller but increases in the gap at the maximum coating thickness will make the system run in a flooded setup instead of fully flooded. At the minimum coating thickness, the web gap could be made smaller to make the coating thickness even thinner, but this will overflow the sides of the gap since the amount of coating on the application coater is at the limit.

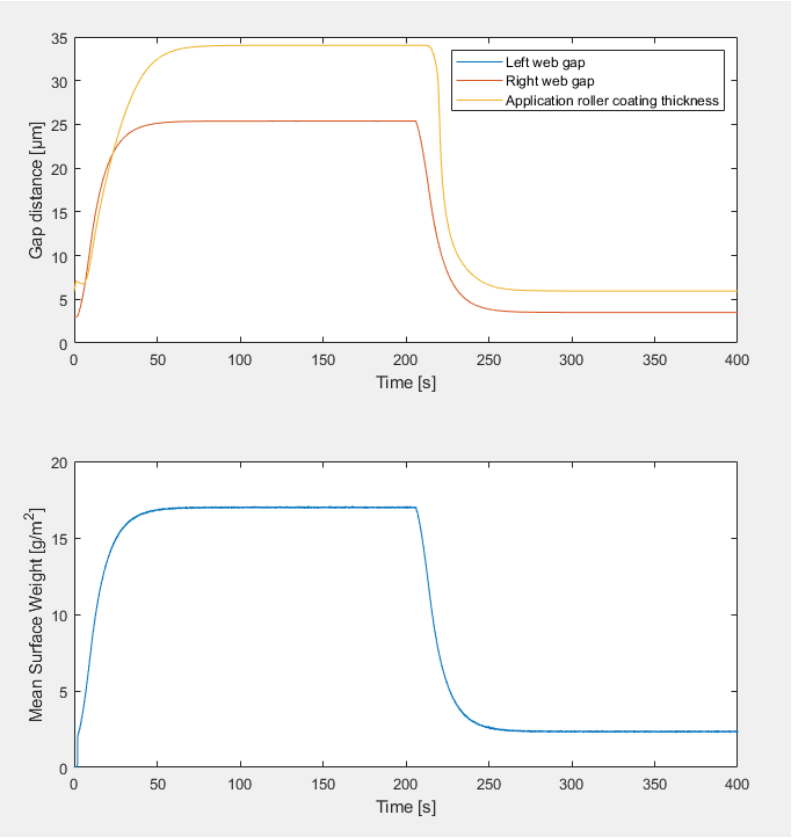

Figure 14: The minimum and maximum coating thickness for the fully flooded configuration at approximately 2.4 and 17 g/m².

4.4.4 Setpoint changes

The following simulation is shown in Figure 15 to illustrate step changes in surface weight for a fully flooded roll coater. The surface weight step point is set to 6 g/m^2 initially and is then changed to 10, 16 and 4 g/m^2. The left figure illustrates the gap change and the application roller coating thickness. After approximately one minute, the system is stable. The step changes are fast in general when the value change is small. The system will take longer to become stable when the change is more significant, as shown when changing from 16 to 4 g/m^2. Depending on the settings on the controller, even faster changes are possible but will also produce more oscillating before reaching stability.

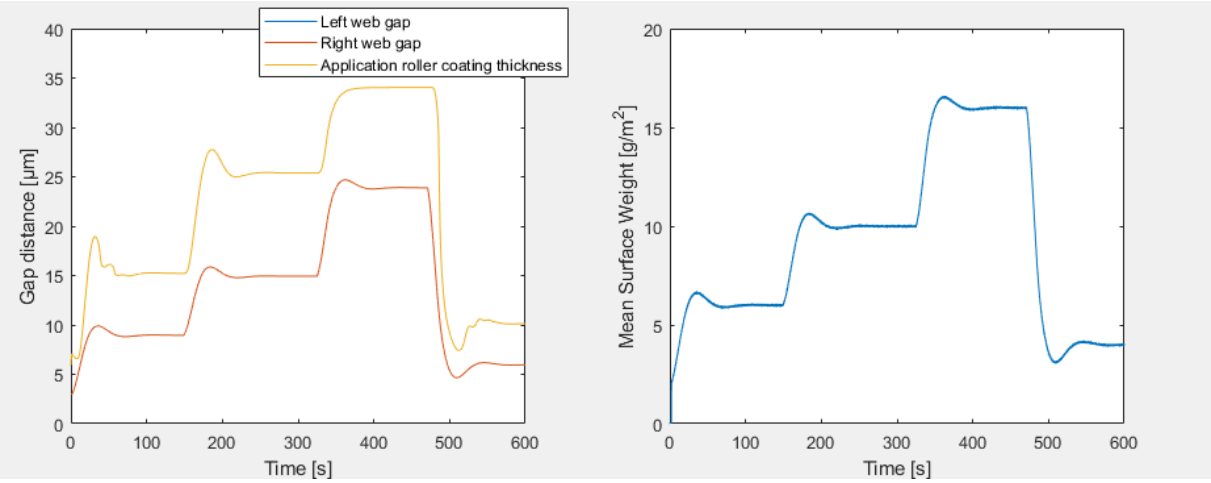

Figure 15: Fully flooded simulation with coating thickness setpoint changed from 6,10,16 to 4 g/m².

4.4.5 Comparison of data between plant and simulation

Coating data from the plant is presented in Figure 16. The application and web roller's speed are 21 m/min, with the metering roll set to half of that at 10.5 m/min. The gap between the application roller and the web roller is 110 µm. The negative gap between the metering and application roller is set to $-2\ mm$. The viscosity varies a bit in the plant data but stays around 97 cP towards the end of the run. Both figures show the same data, but the lower one shows the mean surface weight in a two-axis system, compared to the three-axis version above. The jump in data at the start and middle of the data is due to the plant not running. The set point

the operator wanted is assumed to be between $5 - 6\ g/m^2$. It's also not clear whether the plant is running in a fully flooded or starved scenario. The paper thickness is approximately $80 - 100\ \mu m$.

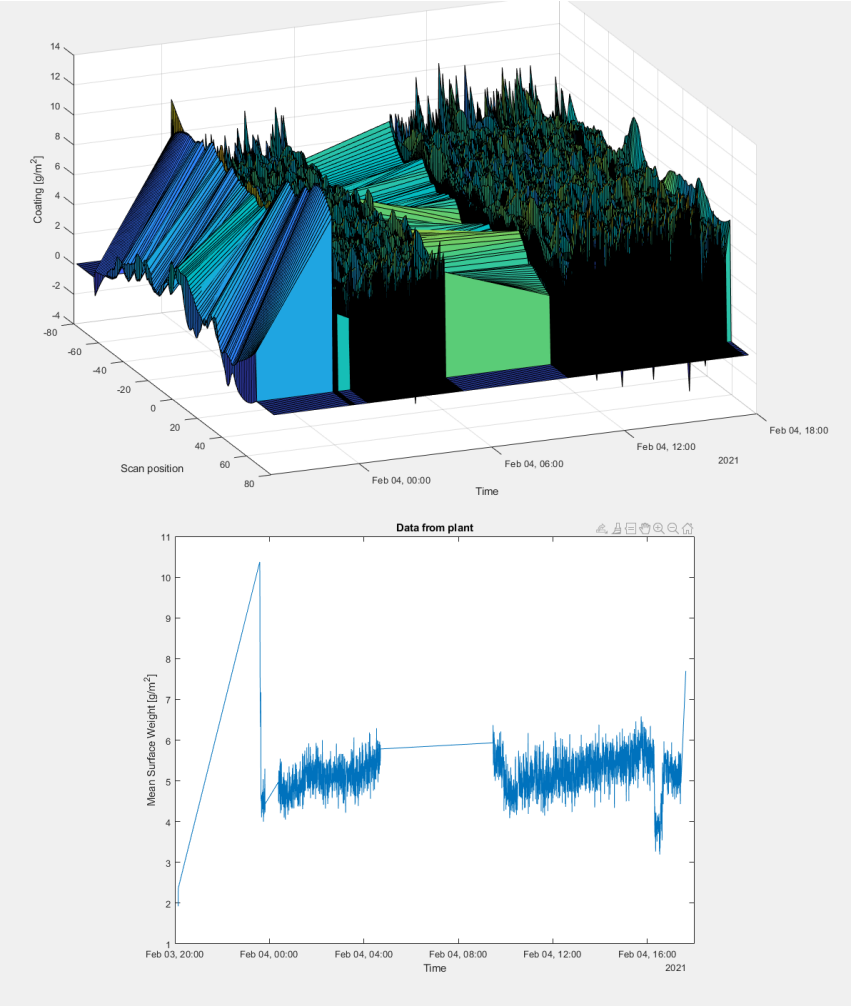

Figure 16: Surface weight data from the plant.

A fully flooded simulation with the surface weight of 5.5 g/m^2 is shown in Figure 17 to represent a similar setpoint as the plant data above. The gap between the application and web roller is presented at approximately $8\ \mu m$ in the top figure. Important to note here is that this does not include the thickness of the paper. This would mean that the combined paper and gap height is around $88 - 108\ \mu m$ compared to the $110\ \mu m$ from the plant. The middle figure shows the mean coating thickness on the paper, with the bottom one showing the

negative gap between the metering roll and application roller. The metering roll gap is around -1.65 mm compared to the -2 mm in the plant data.

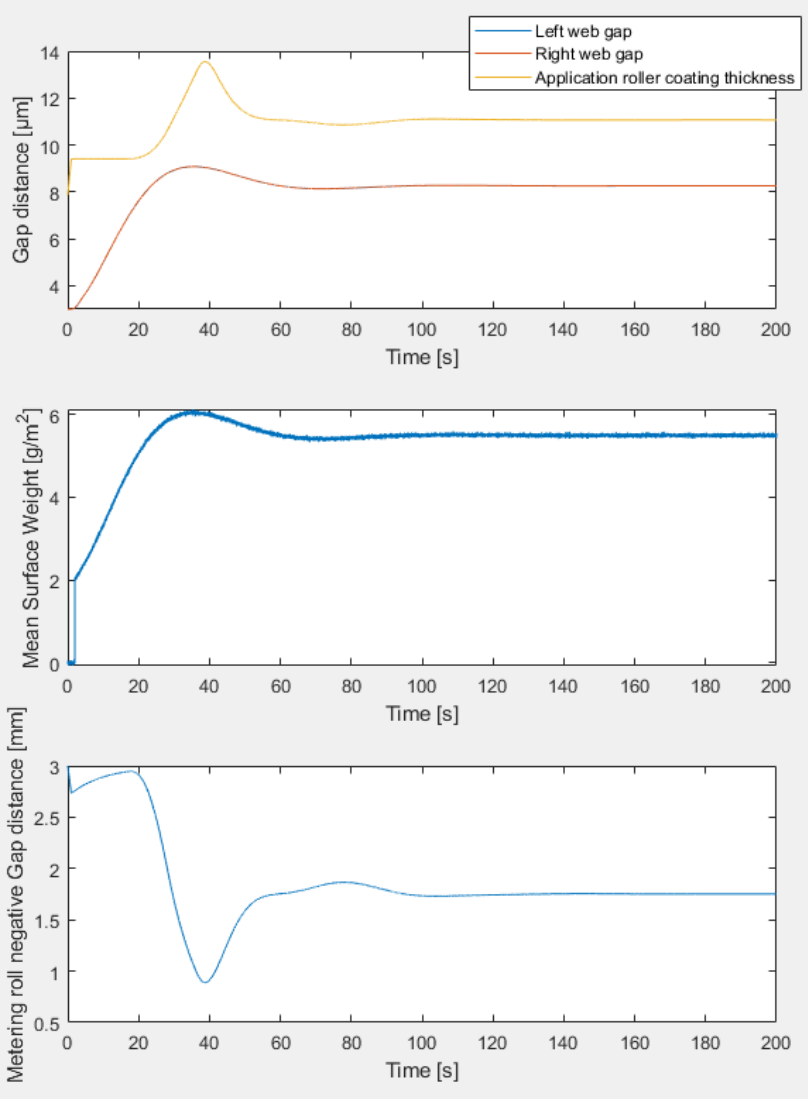

Figure 17: Fully flooded roll coater simulation with same setpoint as plant example. The application coating thickness is set to be 1.34 bigger than the gap, and is therefore bordering the starved regime.

Another simulation is run in Figure 18 with the same surface weight set point as the plant, but the gap is starved instead of fully flooded. The parameter k used for the flow to determine when the starved regime changes to ultra-starved is set to 1.05. For this simulation, the web gap is 5% larger than the application roller coating thickness. The figure uses the same layout as the example above. The top figure shows the gap and the application roller coating thickness, the middle the mean coating thickness on the paper, and the bottom the negative

metering roll gap. The results show that the combined web gap with paper is around 91 – 111 µm, while the negative metering gap is around -1.76 mm.

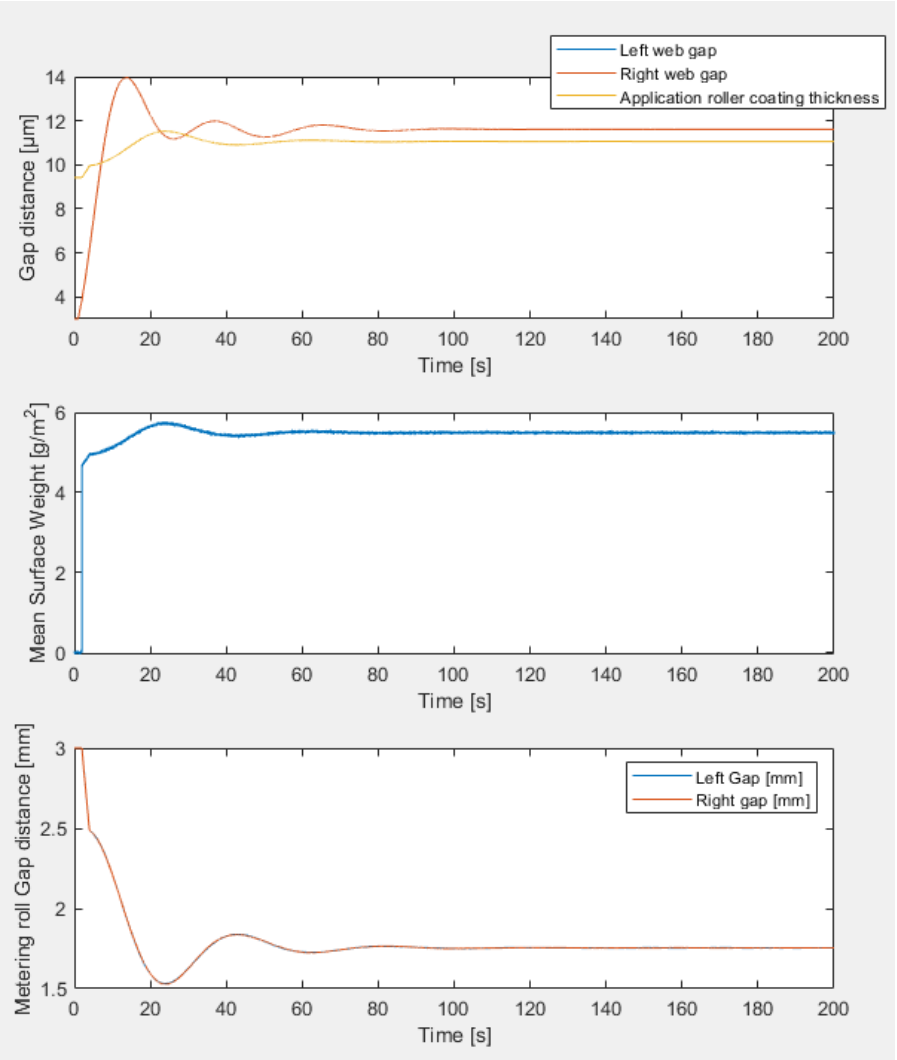

Figure 18: Starved roll coater simulation with same coating set point as plant example. K=1.05 is chosen and the web gap is set to be 5% larger than the application roller coating thickness.

5 Discussion and observations

The approximation assumes the rolls are more or less flat, which should be the case in most plant scenarios. Another thing to note is that it is not the actual width profile presented in the figure, but the zigzag profile, due to the movement of the web and sensor. The sensor will only ever record data from the zigzag pattern, so any width profiles will always be an estimation based on the line approximation and the estimator.

From plant data, it has also been shown that the outer edges of the web will have a thicker coat than the inner parts. This is most likely from the extra coating that is pressed out to the sides of the rolls. In order to get a more accurate representation of the coating thickness, the line approximator is already ignoring the recorded thickness from the web's sides. This thickness discrepancy is most likely to be present when the roller is run in a fully flooded setup due to there being more coating to press out to the sides. The line approximator cuts out the outer data in both the starved and flooded configurations, but this should not be a significant issue because there are more than enough data points to get an accurate representation.

The noise level might also vary in plant scenarios, but there is always noise present, which will impact the accuracy of the measurement. The simulated data points fluctuate a lot due to the noise being Gaussian and added randomly. However, since it is Gaussian and added over a data set, the mean should still be a good representation. The recorded data points from the plant are probably closer to each other compared to the simulated data due to the interaction and properties of the coating fluid.

The effect of the estimator is essential since, without it, there would be no data for most points of the coat. Since the estimator compares data from the simulation with real data points, it should give a good estimation. The only scenario where that is not the case is if the model represents the plant poorly. The model has not been compared extensively with data from the plant because only a small amount of plant data is available.

The line approximation seems to represent how the physical system nicely. This is because there will always be a line between the left and right sides of the rolls and since these are the main actuators affecting the coating thickness, this should be a good approach. A different system might have actuators located in the web to change the local thickness of the coat. This

would give the problem more degrees of freedom and make it more complicated than the studied case. For example, local imperfections from dented rolls could be fixed with such a system. However, such problems are more or less impossible to fix here due to the limitations of the system.

The general accuracy of the model can be assumed to be good from the results shown in Chapter 4.4.5. Similar results are shown in both the fully flooded and starved model when using the same parameters as the plant scenario. Therefore, it is hard to precisely say what regime the plant was running in because both models fit the data. This is partly because there are parameters in both models that can be changed to fit the data. For the fully flooded regime, the amount of extra coating on the application roller was set to be 34% larger than the web gap. This should give a best-case scenario for the fully flooded model. Increasing the application coating thickness will mean that the negative metering gap gets larger and moves further away from the -2 mm that was used in the plant data. On the flip side, making the ratio smaller than 34% will mean that the coater is running in a flooded regime instead of a fully flooded one. For the starved regime, the size of the web gap compared to the application coating thickness can be set alongside the k parameter to make it fit the plant data. Note that the starved regime would fit the plant run better since the negative metering gap is even smaller in the plant data. From observations in the plant, the system is also usually operated in a starved configuration. Comparing more data would be beneficial, but the available data has been low, so more comparisons have been limited. This is mainly because plant visits have not been possible due to the covid-19 epidemic, so gathering specific data applicable to this thesis has been challenging.

For this thesis in particular, interesting data to gather from the plant is when the coating on the application roll loses contact with the paper when operated in a starved setup. Since this is an unknown, there is no system set to handle losing contact with the paper in the current program. Having no system means that if the rollers lost contact, the system would try to increase the amount of coating on the application roller because of the feedback response. A solution to this could be first to investigate how large the web and application gap can be before losing contact. Then this could be calculated backward to get a limiting ratio between the metering and application system and the web and application system to ensure that the contact is never lost. Procuring a ratio is needed because the amount of coating on the

application roller is not measured and can therefore not be used as a feedback response unless estimated.

Another thing that could be beneficial from an academic point of view is to figure out is how the gap behaves when swapping from one regime to another. The proposed flow equations presented in Chapters 2.2.3 and 2.2.5 are implemented to ensure that the flow rate change is gradual between the regimes. This seems logical since in reality, the changes in flow between regimes are probably more or less continuous when going from one regime to another. However, investigating this phenomenon might not be that interesting from an industry or plant point of view since the plant is most likely run with either one regime or the other and not going in between regimes.

An important note to remember is that even if the model does not exactly represent how the system behaves, the controller will still achieve the desired setpoint due to how a feedback control system works. That is one of the best perks of using a feedback system in any control system in general.

Currently, the plant is using operators that manually control the plant's parameters. Using a feedback control system instead has several advantages. Firstly, the controller output will constantly try to reduce the error of the plant and will therefore reduce the plant’s dynamic disturbances. A human operator will have a more challenging time keeping up with all the minor disturbances that are constantly happening. Secondly, changing set points of the plant should be much faster with a feedback loop. In most simulations, finding the correct gap heights is usually done in around one minute. Manual operating takes a significantly longer time to get the desired result.

This thesis focuses on the model implementation and control of the system. The next step would be to continue building models for the rest of the plant and connect them to the physical systems. This will then make it possible to get a full-scale digital representation of how everything in the plant runs, or in other words, a digital twin. The advantage of using a virtual twin is that it can analyze and make intelligent decisions for the whole process by simulation instead of factory testing. Digital twins can optimize the whole plant to the best settings to maintain optimal performance. Component replacement intervals can also be optimized by running predictive diagnoses in the digital space.

6 Conclusions

The simulations show that the model corresponds well compared to plant data. Plant visits have not been possible due to the Covid-19 epidemic, so gathering data have been difficult. An interesting phenomenon that still needs to be studied is when the coating loses contact with the web when operating in a starved configuration.

For the methods implemented to control the system, the line approximation is a good representation of how the physical system will behave due to the geometry of the rolls. The estimator is essential to ensure that data is available when the sensor is not present. The feedback loop will make sure that correct setpoints are achieved, even if the model might differ a bit from reality. It will also minimize the effect of plant disturbances and improve plant productivity by making step changes faster than manual control.

The next step is to connect the model to the physical space and continue adding other pieces of the plant to the model. This will create a digital twin of the whole plant and digitally represent the physical system. Using digital twins as a testing environment will save both time and money compared to running plant tests.

References

Abbott, S. et al., 2011. A review of the fluid mechanics of rigid roll coating systems. *Convert & e-Print,* Volume 1, pp. 47-51.

Carvalho, M. S. & Scriven, L. E., 1997. Deformable roll coating flows: steady state and linear perturbation analysis. *Journal of Fluid Mechanics,* pp. vol. 339: 143-172.

Chong, Y., Gaskell, P. & Kapur, N., 2007. Coating with deformable rolls: An experimental investigation of the ribbing instability. *Chemical Engineering Science 62,* pp. 4138-4145.

Cognard, P., 2006. *Handbook of Adhesives and Sealants, Volume 2.* s.l.:Elsevier Science.

Cohu, O. & Magnin, A., 1997. Forward roll coating of Newtonian fluid with deformable rolls: an experimental investigation. *Chemical Engineering Science,* 52(8), pp. 1339 - 1347.

Coyle, D., 1997. Liquid Film Coating. In: s.l.:Chapman & Hall, p. Chapter 12a.

Gaskell, P., Savage, M. & Thompson, H., 1998. Stagnation-saddle points and flow patterns in Stokes flow between contra-rotating cylinders. *Journal of Fluid Mechanics,* Volume 370, pp. 221-247.

Häggblom, K.-E. & Böling, J., 2013. *Reglerteknik 2.* Åbo, Finland: Åbo Akademi - Department of chemical engineering.

Johnson, M. A., 2003. *Viscoelastic Roll Coating Flows,* Maine: University of Maine.

Kapur, N., 1999. *Flow phenomena in Fixed-Gap and Gravure roll coating systems.* Leeds: The University of Leeds.

Landau, L. & Levich, B., 1942. Dragging of a liquid by a moving plate. *Acta Physicochim, (USSR),* Volume 17, pp. 42-54.

MathWorks, 2022. *https://www.mathworks.com.* [Online]
Available at: https://www.mathworks.com/help/curvefit/least-squares-fitting.html
[Accessed 25 January 2022].

Tao, F., Zhang, H., Nee, A. Y. C. & Liu, A., 2019. Digital Twin in Industry: State-of-the-Art. *IEEE Transactions on industrial informatics,* 15(4), pp. 2405-2415.

Thompson, H. M., 1992. *A theoretical investigation of roll coating phenomena.* Leeds: University of Leeds.

VanAntwerp, J. G., Featherstone, A. P., Braatz, R. D. & Ogunnaike, B., 2007. Cross-directional control of sheet and film processes. *Automatica,* 43(3), pp. 191-211.

Wells, D. E. & Krakiwsky, E. J., 1971. *The method of least squares.* New Brunswick, Canada: University of New Brunswick.